SnS Quantum Dots – A Green Photovoltaic Material

Sakshi Chaudhary[1] and Salam Samarendra Singh[2]
[1]Department of Physics, D. J. College, Baraut, U. P. -250611, India
[2]Department of Mathematics, G.P.Women's College, Imphal, Manipur – 795001, India
Email of corresponding author: sakshichaudhary950@gmail.com

Structures and electronic properties of SnS quantum dots (QDs) are studied by using first principles density functional theory (DFT) for their potential applications in the design of environmentally friendly green solar cells. QDs of different sizes are investigated and effect of ligation on geometry optimization and the electronic properties of the QDs are investigated. Also, effect of stoichiometry of the QDs is also investigated. There is a red shift on the absorption peak of the QDs as the size of QDs is increased.

Keywords: Quantum dots, solar cells, DFT.

1. INTRODUCTION

Narrow band gap applications of near-infrared (NIR) and infrared (IR) optically active IV-VI semiconductor nano-particles (NPs) like PbS, SnTe, and SnS are of significant interest. As such, strong IR absorption is necessary in photovoltaics, near-infrared detectors, and medical applications [1]. These applications have sparked research into practical synthetic techniques for producing SnS NPs with precise optical characteristics and restricted size distributions and also because of their non-toxic properties. Due to their simplicity of synthesis, monodispersed chalcogenide nanocrystals having cubic configurations like CdS, CdSeS, CdSe, PbS, and SnTe have received a lot of interest in the last 20 years [2]. The crystal structure of SnS is an orthorhombic layered structure that resembles a warped version of the NaCl structure [3]. SnS exists in three form as zinc blende, rock salt and orthorhombic form at high temperature. Sulphides of tin can be found in a variety of chemical forms, including SnS, SnS_2, and Sn_2S_3 [4]. SnS_2 has 2.36 eV indirect bandgap and an n-type character. When other phases, such as SnS_2, SnS_3, etc., are present with SnS material under suboptimal deposition circumstances, the bandgap shifts to higher energies. It has also been claimed that zinc blende (ZB) SnS exists in the form of particles and thin films [5], which might create a pure interface in a solar cell with zinc blend structure of CdS. Their optical absorption efficiency is quite significant with linear bandgap. Although simulations indicate that ZB SnS is unreliable from thermodynamic and dynamical perspective, studies of ZB SnS tiny particles, being created and fabricated as thin films, suggest that these materials are practically viable to create. Devices such as photodetectors, equipped with ribbon crystalline SnS, have been realised. All vacuum and non-vacuum fabrication processes are capable of producing thin-film SnS. The methods of preparation include spray pyrolysis [6], thermal decomposition [7,8,9], chemical vapour deposition (CVD) [10], chemical bath deposition (CBD) [11-14], pulsed CVD [15] etc. SnS solar cells can achieve the efficiency of Shockley- Queisser limit of 31%, compared to a prior theoretical maximum conversion

efficiency estimate of 25%. According to device simulation using the materials' data, a-Si/SnS and ZnS/SnS heterojunctions can provide output with respective efficiencies of 14.30% and 16.2%.[16] Additionally, it is hypothesised that one of the causes of the subpar properties of SnS cells is the defect formation brought on by Sn vacancies. It is unclear if the SnS QDs will also experience the same defect creation mechanism. The defect-free bulk (QD interior) is maintained by pushing the defects to the particle borders, which is energetically advantageous. By using proper ligands, a shell, or by incorporating the boundary into a passivating matrix, the boundary can be passivated. SnS NPs are currently being investigated for both organic as well as inorganic solar cells applications [17]. The present work focuses on SnS QDs as a highly promising solar cell material and effect of sizes of the QDs and their stoichiometry have been investigated.

2. COMPUTATIONAL & SIMULATION DETAILS

2.1. Model Systems

The QDs (stoichiometric and off-stoichiometric) under study are shown in the Figure 1. Methyl ammonium (MA) and iodide (I^-) radicals were utilised as passivating agents at the surface of these QDs. The number of iodide radicals to be coupled to each QD is determined by the system's charge neutrality. These MA/iodide ions were anchored at four suitable sites at the surface of each of the SnS QDs of various constitutions (off-stoichiometric) in order to make the QD charge neutral. For stoichiometric QDs, equal numbers of iodide and MA ions are attached for surface passivation. Further, these SnS QDs under study are taken of different sizes with different composition of Sn, S and iodide ions. To make $Sn_{14}S_{16}$ QDs electrically neutral, four MA (methyl ammonium) radicals were added to the QD and in case of $Sn_{16}S_{14}$ four iodide ions were added at appropriate sites. An earlier work used a similar approach to produce charge neutral QDs [18].

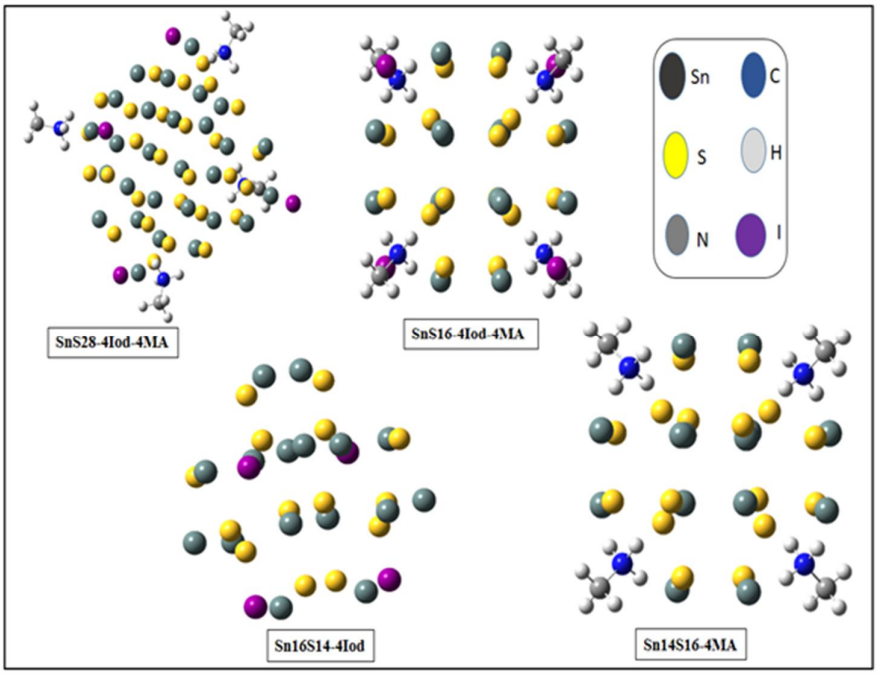

Fig. 1: Optimised Structure of model QDs ligated with Methyl Ammonium, and Iodide

2.2. Computational Details

Our calculations, based on first principles density functional theory (DFT), made use of a hybrid functional (CAM-B3LYP) [19,20] and for basis sets the 6-311G(d,p) [21]/LANL2DZ [22] are used, implemented in the Gaussian 09 software package [23]. To describe the H, C, and N atoms the 6-311G(d,p) basis set was used, the effective core potentials with a double-zeta valence basis set (LANL2DZ) were utilised to describe the Sn, S, and I atoms. Without symmetry restrictions, the geometry of each cluster was optimised till the remaining forces were below 0.00045 a.u. The projected densities of states (PDOS) of various constituent atoms/radicals/ligands in the systems were determined using the AOMIX package. In order to avoid issues with atomic charge assignment in the Mulliken population analysis using the large basis set, the computation of the projected density of states (PDOS) was done using a double-zeta-polarized (DZP) basis set [24-27]. And a gaussian function with a 0.5eV half-width at half-maximum (HWHM) was used for the PDOS convolution for each QD. The same level of accuracy, as mentioned above in DFT calculation, is used in TDDFT calculations so that we can compute the absorption spectrum. Calculation for the vertical excitation energies (excluding zero point energies) and oscillator strengths were done at the ground state geometries and a gaussian function with HWHM of 0.1eV and it is used for the computation of the convolution of the absorption spectra. Lastly, Natural transition orbitals (NTOs) analyses are used to comprehend how charges are transferred throughout the system during absorption. The NTO analysis is trustworthy because for the electronic transition density matrix, it uses a

small orbital representation. There is a correlation between the excited particle and the empty hole thanks to the independent unitary transformations of the occupied and virtual orbitals [28].

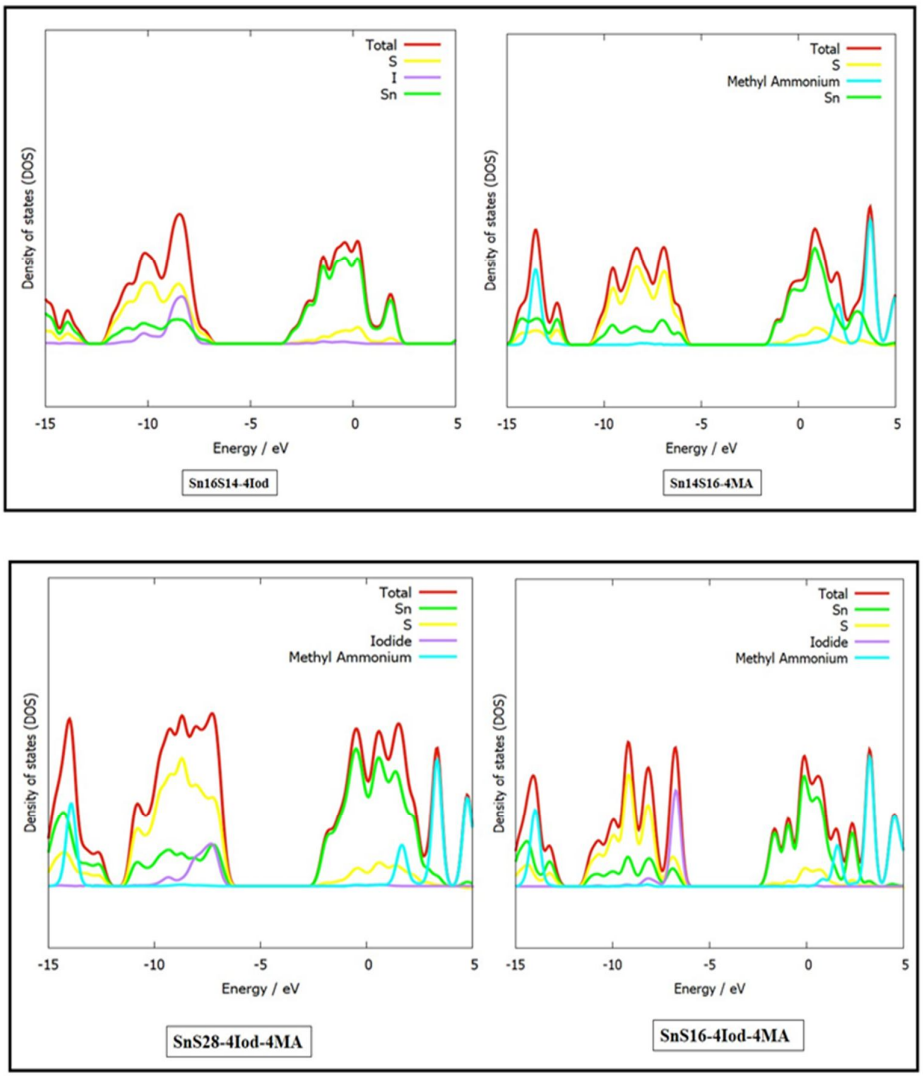

Fig. 2: PDOS for (A) $Sn_{16}S_{14}$ (B) $Sn_{14}S_{16}$ (C) SnS_{28} and (D) SnS_{16} ligated with iodide and MA ions.

3. RESULTS AND DISCUSSIONS

3.1. PDOS Analysis

The contribution of various atoms in HOMO (Highest occupied molecular orbital) and LUMO (Lowest unoccupied molecular orbital) can be assessed in PDOS analysis. From PDOS curves (Figure 2), it is clearly visible that S contributes maximum in HOMO and LUMO lies on Sn in all cases although in case of $Sn_{16}S_{14}$ ligated with 4 iodide the HOMO lies on I and LUMO on Sn. Also, in case of $Sn_{14}S_{16}$ ligated with methyl ammonium (MA) the contribution of MA is not seen or we can say that energy levels corresponding to MA are completely buried in the energy bands for this model QD. There is no CH_3NH_3 contribution to either the HOMO or LUMO in both stoichiometric SnS_{16} and SnS_{28} QDs.

Table 1: Optical Excitation Data of model systems using TDDFT for some important transitions.

Model System	ES Transition	Oscillatory Strength	Wavelength (nm)	Energy (eV)
Sn14S16-4MA	$S_0 \rightarrow S_{44}$	0.0346	303.58	4.0840
	$S_0 \rightarrow S_{43}$	0.0272	304.23	4.0753
	$S_0 \rightarrow S_{25}$	0.0251	328.23	3.7774
	$S_0 \rightarrow S_1$	0.0237	423.22	2.9295
Sn16S14-4Iod	$S_0 \rightarrow S_{46}$	0.0282	319.94	3.8752
	$S_0 \rightarrow S_{36}$	0.0270	329.84	3.7584
	$S_0 \rightarrow S_2$	0.0281	475.45	2.6077
	$S_0 \rightarrow S_1$	0.0186	534.00	2.3218
SnS16-4Iod	$S_0 \rightarrow S_{23}$	0.0101	384.22	3.2269
	$S_0 \rightarrow S_{24}$	0.0101	384.22	3.2269
	$S_0 \rightarrow S_{25}$	0.0101	384.22	3.2269
SnS28-4Iod	$S_0 \rightarrow S_{39}$	0.0142	382.99	3.2372
	$S_0 \rightarrow S_{40}$	0.0142	382.98	3.2373
	$S_0 \rightarrow S_{41}$	0.0140	382.92	3.2379

3.2. Absorption Spectra

Figure 3 and 4 shows the absorption spectra of all the four SnS QDs under study. We observed that the absorption starts at 1.8 ev and goes on till 4.9 eV. In case of Sn14S16-4MA the peak lies at 3.9eV and absorption lies in the range of 2.2 to 4.9eV. For Sn16S14-4I the absorption peak is found at 3.7 eV and ranging from 1.8 to 4.6 eV similarly for Symmetrical QDs i.e. SnS_{16} and SnS_{28} ligated with 4 Iodide and 4 Methyl Ammonium the peaks lies at 3.25 and 3.1 eV respectively. Furthermore, the absorption starts around 2.3eV and goes on till 4.2eV for SnS_{16} and in case of SnS_{28} QD this range happens to be 1.8 to 4 eV.

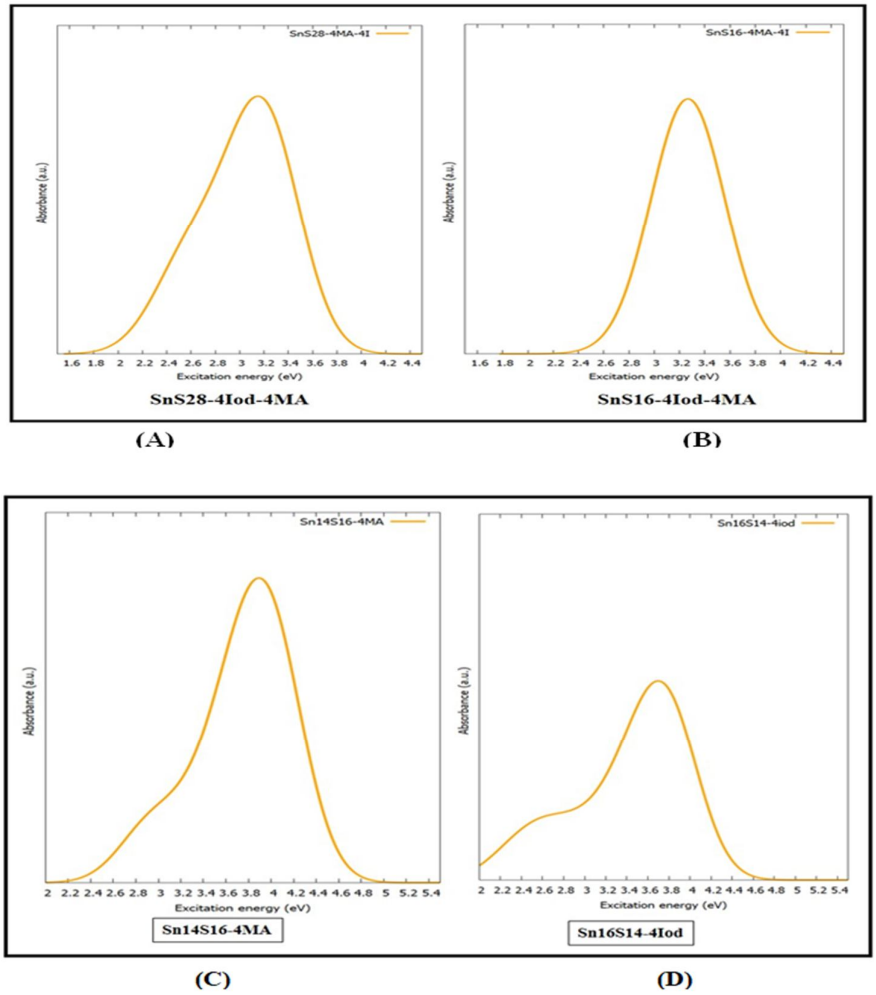

Fig. 3: Optical absorption spectra of (A) SnS_{28} (B) SnS_{16} (C) $Sn_{14}S_{16}$ ligated with 4 Methyl Ammonium (D) $Sn_{16}S_{14}$ ligated with 4 Iodide radicals.

3.3 NTO Analysis

Analysing the NTO in Figure 4 gives the charge transfer pattern in each QD in every case the hole charge density distribution in the ground state is given on left side and the electron charge density distribution in the excited state is given on right side.

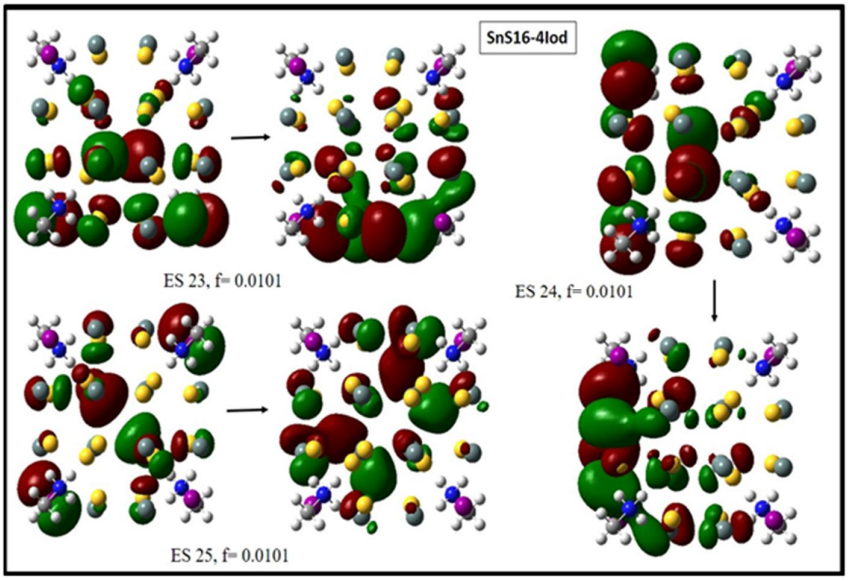
SnS16-4Iod
ES 23, f= 0.0101
ES 24, f= 0.0101
ES 25, f= 0.0101

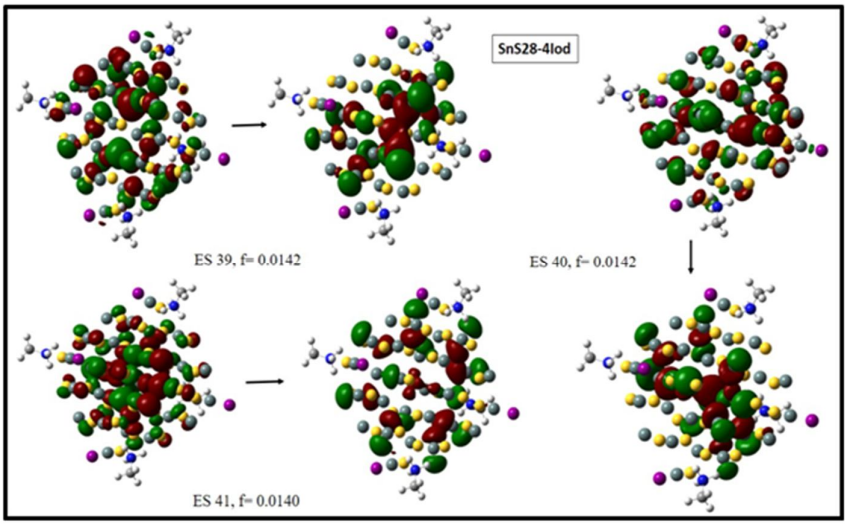
SnS28-4Iod
ES 39, f= 0.0142
ES 40, f= 0.0142
ES 41, f= 0.0140

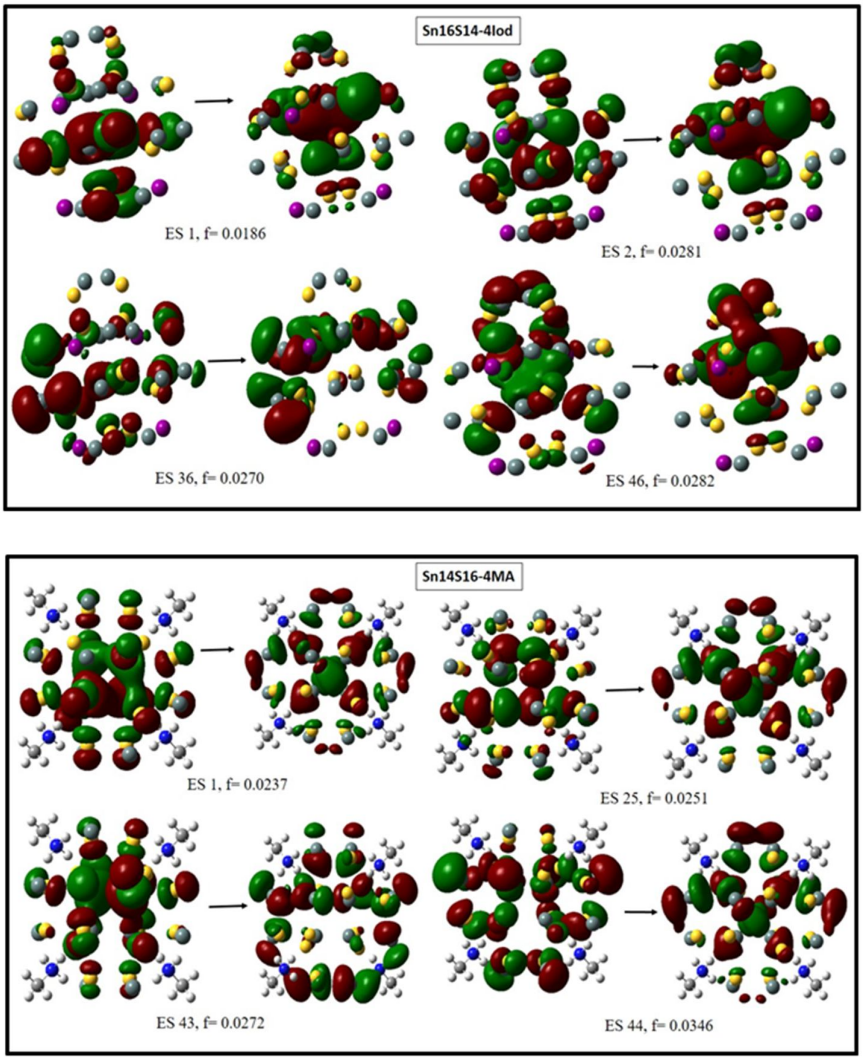

Fig. 4: Natural Transition Orbitals (NTOs) of few selected excited states of SnS QDs.

It is seen that the charge transfer takes place from p orbital of S and I in ground state to p orbital of Sn and S charge distribution left with S in almost all cases. In case of SnS_{16} ligated with 4MA and 4 iodide ions, the charge is sometimes distributed on half portion of QD sometimes it is moving from central part of QD to outer portion of QD. In case of SnS-28 the pattern of charge transfer is transverse as well as from centre of the QD to outward. Similarly shifting of charge cloud from p of S to P of Sn with a small contribution of p type charge cloud around I in ground state is seen in case of $Sn_{16}S_{14}$ ligated with 4 Iodide. The charge transfer is very good and accumulating around one end of the QD. Further in case of $Sn_{14}S_{16}$ ligated with 4 MA the charge is shifting from inside to outside

and also from one end of the QD to opposite side of QD from p of S in ground state to p of Sn in excited state.

4. CONCLUSION

From the DFT study of a few SnS QDs, both stoichiometric and off-stoichiometric, it is found that there are charge transfer transitions in many of these systems although the corresponding oscillator strengths of these transitions are not strong. This may be because of the passivating agents on the surface of these QDs. There is a red shift in the absorption peak of the QDs as the size of the QD is increased, both in stoichiometric and off-stoichiometric QDs. These SnS QDs may be used as active material in environmental friendly green solar cell systems.

5. ACKOWLEDGEMENT

The authors are thankful to Dr. Shyam Kishor for providing computing facility and for providing the Gaussian 09 software package and other softwares for simulation work. Also, they are thankful to Dr. Kh. S. Singh for valuable suggestions during the course of this work.

REFERENCES

[1] T. Rauch, M. Boberl, S.F. Tedde, J. Furst, M.V. Kovalenko, G. Hesser, U. Lemmer, W. Heiss and O. Hayden; “Near-infrared imaging with quantum-dot-sensitized organic photodiodes”, Nature Photonics, Vol. 3, pp. 332-336, 2009.

[2] Y. Xu, N. Al-Salim, C.W. Bumby and R.D. Tilley; “Synthesis of SnS Quantum Dots”, Journal of American Chemical Societ, Vol. 131(44), pp. 15990–15991, 2009.

[3] J.M. Chamberlain, P.M. Nikolic, M. Merdan and P. Mihailovic; “Far-infrared optical properties of SnS”, Journal of Physics C: Solid State Physics, Vol. 9, pp. L637-L642, 1976.

[4] L.A. Burton and A. Walsh; “Phase stability of the earth-abundant tin sulfides SnS, SnS_2, and Sn_2S_3”, J. Phys. Chem. C, Vol. 116(45), pp. 24262– 24267, 2012.

[5] E.C. Greyson, J.E. Barton and T.W. Odom; “Tetrahedral Zinc Blende Tin Sulfide Nano- and Microcrystals”, Small, Vol. 2(3), pp. 368–371, 2006.

[6] K.T.R. Reddy, N.K. Reddy and R.W. Miles; “Photovoltaic Properties of SnS Based Solar Cells”, Solar Energy Materials and Solar Cells, Vol. 90(18-19), pp. 3041-3046, 2006.

[7] M. Devika, N.K. Reddy, K. Ramesh, V. Ganesan, E.S.R. Gopal and K.T.R. Reddy; “Influence of substrate temperature on surface structure and electrical resistivity of the evaporated tin sulphide films”, Appl. Surf. Sci., Vol. 253(3), pp. 1673–1676, 2006.

[8] R.W. Miles, O.E. Ogah, G. Zoppi and I. Forbes; “Thermally evaporated thin films of

SnS for application in solar cell devices", Thin Solid Films, Vol. 517(17), pp. 4702-4705, 2009.

[9] M.M. El-Nahass, H.M. Zeyada, M.S. Aziz and N.A. El-Ghamaz; "Optical Properties of thermally evaporated SnS Thin films", Opt. Mater., Vol. 20(3), pp.159–170, 2002.

[10] A.T. Kana, T.G. Hibbert, M.F. Mahon, K.C. Molloy, I.P. Parkin and L.S. Price; "Organotin unsymmetric dithiocarbamates: synthesis, formation and characterisation of tin(II) sulfide films by atmospheric pressure chemical vapour deposition", Polyhedron, Vol. 20(24-25), pp. 2989–2995, 2001.

[11] E. Guneri, C. Ulutas, F. Kirmizigul, G. Altindemir, F. Gode, and C. Gumus; "Effect of deposition time on structural, electrical, and optical properties of SnS thin films deposited by chemical bath deposition", Applied Surface Science, Vol. 257(4), pp. 1189-1195, 2010.

[12] P.K. Nair, M.T.S. Nair, V.M. Garcia, O.L. Arenas, Y. Pena, A. Castillo, I.T. Ayala, O. Gomezdaza, A. Sanchez, J. Campos, H. Hu, R. Suarez and M.E. Rincon; "Semiconductor Thin Films by Chemical Bath Deposition for Solar Energy Related Applications", Solar Energy Materials and Solar Cells, Vol. 52(3-4), pp. 313-344, 1998.

[13] M. Leach, K.T.R. Reddy M.V. Reddy. J.K. Tan, D.Y. Jang and R.W. Miles; "Tin Sulphide Thin Films Synthesised using a Two Step Process", Energy Procedia, Vol. 15, pp. 371-378, 2012.

[14] A. Akkari, C. Guasch and N. Kamoun; "Optical studies and structural properties of chemically deposited tin sulphide", 23rd European Photovoltaic Solar Energy Conference and Exhibition, Valencia, Spain, pp. 477-480, 2008.

[15] L.A. Burton and A. Walsh; "Band alignment in SnS thin-film solar cells: Possible origin of the low conversion efficiency", Appl. Phys. Lett., Vol. 102, pp. 132111, 2013.

[16] J.J. Loferski; "Theoretical Considerations Governing the Choice of the Optimum Semiconductor for Photovoltaic Solar Energy Conversion", J. Appl. Phys., Vol. 27(7), pp. 777, 1956.

[17] F. Tan, S. Qu, J. Wu, K. Liu, S. Zhou and Z. Wang; "Preparation of SnS_2 colloidal quantum dots and their application in organic/inorganic hybrid solar cells", Nanoscale Res. Lett., Vol. 6, Article number 298, 2011.

[18] M. Del Ben, R.W.A. Havenith, R. Broer and M. Stener; "Density functional study on the morphology and photoabsorption of CdSe nanoclusters", J. Phys. Chem. C, Vol. 115(34), pp. 16782-16796, 2011.

[19] P.J. Stephens, F.J. Devlin, C.S. Ashvar, C.F. Chabalowski and M.J. Frisch; "Theoretical calculation of vibrational circular dichroism spectra", Faraday Discussions, Vol. 99, pp. 103-119, 1994.

[20] T. Yanai, D.P. Tew and N.C. Handy; “A new hybrid exchange–correlation functional using the Coulomb-attenuating method (CAM-B3LYP)”, Chemical Physics Letters, Vol. 393(1-3), pp. 51-57, 2004.

[21] W.J. Hehre, R. Ditchfield and J.A. Pople; “Self-Consistent Molecular Orbital Methods. XII. Further Extensions of Gaussian-Type Basis Sets for Use in Molecular Orbital Studies of Organic Molecules”, J. Chem. Phys., Vol. 54, pp. 2257, 1972.

[22] S. Chiodo, N. Russo and E. Sicilia; “LANL2DZ basis sets recontracted in the framework of density functional theory”, J. Chem. Phys., Vol. 125, pp. 104-107, 2006.

[23] M.J. Frisch, et al. Gaussian 09, Revision C.01; Gaussian, Inc.; Willingford, CT, 2011.

[24] A.C. Neto, E.P. Muniz, R. Centoducatte and F.E. Jorge; “Gaussian basis sets for correlated wave functions. Hydrogen, helium, first- and second-row atoms”, J. Mol. Struct. (Theochem), Vol. 718(1-3), pp. 219-224, 2005.

[25] G.G. Camiletti, S.F. Machado and F.E. Jorge; “Gaussian basis set of double zeta quality for atoms K through Kr: application in DFT calculations of molecular properties”, J. comput chem., Vol. 29(14), pp. 2434-2444, 2008.

[26] S.I. Gorelsky; “AOMix: Program for Molecular Orbital Analysis”, http://www.sg-chem.net/, 2013, version 6.80.

[27] S.I. Gorelsky and A.B.P. Lever; “Electronic structure and spectra of ruthenium diimine complexes by density functional theory and INDO/S. Comparison of the two methods”, J. Organomet. Chem., Vol. 635(1-3), pp. 187-196, 2001.

[28] R.L. Martin; “Natural Transition Orbitals”, J. Chem. Phys., Vol. 118, pp. 4775-4477, 2003.